Author Manuscript

Author Manuscript

Author Manuscript

Author Manuscript

HHS Public Access

Author manuscript

Oncogene. Author manuscript; available in PMC 2016 May 18.

Published in final edited form as:

Oncogene. 2016 February 11; 35(6): 702–714. doi:10.1038/onc.2015.117.

Androgen Signaling Is a Confounding Factor for β-catenin-mediated Prostate Tumorigenesis

Suk Hyung Lee[1], **Richard Luong**[2], **Daniel T. Johnson**[1], **Gerald R. Cunha**[3], **Leena Rivina**[1], **Mark L. Gonzalgo**[1], and **Zijie Sun**[1,*]

[1]Department of Urology, Stanford University School of Medicine, Stanford, CA 94305

[2]Department of Comparative Medicine, Stanford University School of Medicine, Stanford, CA 94305

[3]Department of Urology, School of Medicine, University of California San Francisco, San Francisco, CA 94143

Abstract

Emerging evidence has demonstrated the critical roles for both androgen and Wnt pathways in prostate tumorigenesis. A recent integrative genomic analysis of human prostate cancers has revealed a unique enrichment of androgen and Wnt signaling in early onset prostate cancers, implying their clinical significance in the disease. Additionally, interaction between the androgen receptor (AR) and β-catenin has long been detected in prostate cancer cells. However, the consequence of this interaction in prostate tumorigenesis is still unknown. Because mutations in adenomatous polyposis coli (APC), β-catenin, and other components of the destruction-complex are generally rare in prostate cancers, other mechanisms of aberrant Wnt signaling activation have been speculated. To address these critical questions, we developed *Ctnnb1*$^{L(ex3)/+}$*/R26hAR*$^{L/+}$*:PB-Cre4* mice, in which transgenic AR and stabilized β-catenin are co-expressed in prostatic epithelial cells. We observed accelerated tumor development, aggressive tumor invasion, and a decreased survival rate in *Ctnnb1*$^{L(ex3)/+}$*/R26hAR*$^{L/+}$*:PB-Cre4* compound mice compared to age-matched *Ctnnb1*$^{L(ex3)/+}$*:PB-Cre4* littermate controls, which only have stabilized β-catenin expression in the prostate. Castration of the above transgenic mice resulted in significant tumor regression, implying an essential role of androgen signaling in tumor growth and maintenance. Implantation of the prostatic epithelial cells isolated from the transgenic mice regenerated PIN and prostatic adenocarcinoma lesions. Microarray analyses of transcriptional profiles showed more robust enrichment of known tumor and metastasis promoting genes: Spp1, Egr1, c-Myc, Sp5, and Sp6 genes in samples isolated from *Ctnnb1*$^{L(ex3)/+}$*/R26hAR*$^{L/+}$*:PB-Cre4* compound mice than those from *Ctnnb1*$^{L(ex3)/+}$*:PB-Cre4* and *R26hAR*$^{L/+}$*:PB-Cre4* littermate controls. Together, these data demonstrate a confounding role of androgen signaling in β-catenin initiated oncogenic transformation in prostate tumorigenesis.

Users may view, print, copy, and download text and data-mine the content in such documents, for the purposes of academic research, subject always to the full Conditions of use:http://www.nature.com/authors/editorial_policies/license.html#terms

*To whom correspondence should be addressed: Zijie Sun, Ph.D, MD, S221, Grant Building, Stanford University School of Medicine, Stanford, CA 94305-5328, Tel: 650-498-7523, Fax: 650-725-8502, ; Email: zsun@stanford.edu

CONFLICT OF INTEREST: The authors declared no conflict competing financial interest in relation to this study.

Author Manuscript Author Manuscript Author Manuscript Author Manuscript

Keywords

Wnt signaling; β-catenin; androgen receptor; prostate cancer; animal models

INTRODUCTION

Androgen signaling, mediated through the androgen receptor (AR) and its ligands, testosterone and 5α-dihydrotestosterone (DHT) is essential for prostate tumorigenesis[1–3]. Androgen deprivation therapy inhibits androgen-signaling mediated cell growth and survival and thus has been widely used to treat prostate cancer (PCa)[4]. The AR is expressed in most prostate cancer samples before and after the therapy[5]. In fact, *AR* gene amplification appears in one-third of PCa samples after androgen deprivation therapy[6]. Additionally, global gene expression profiling shows that the *AR* is one of several genes to be consistently up-regulated in castration resistant prostate cancer (CRPC)[7, 8], underscoring the significance of androgen signaling in prostate tumorigenesis.

Likewise, Wnt signaling pathways play a significant role in prostate tumorigenesis[9]. Abnormal expression of Wnt ligands, receptors, and effectors has been identified in PCa cells and cells of the surrounding microenvironments, suggesting paracrine regulatory mechanisms in prostate tumorigenesis[10, 11]. In the canonical signaling pathway, secreted Wnt ligands bind to Frizzled proteins and regulate the stability of β-catenin, a key component of Wnt signaling[12]. In the absence of a Wnt signal, β-catenin is constitutively down-regulated by a multicomponent destruction complex containing glycogen synthase kinase 3β (GSK3β), axin, and adenomatous polyposis coli (APC), promoting phosphorylation on serine and threonine residues in the N-terminal region of β-catenin following "priming" phosphorylation of Ser45 by Casein Kinase I (CKI), and thereby targeting it for degradation via the ubiquitin proteasome pathway[13–16]. Increase in nuclear β-catenin has been shown to promote PCa cell proliferation[17]. In mice, expression of stabilized β-catenin in the prostate induces the development of squamous metaplasia, prostate intraepithelial neoplasias (PIN)[18, 19], and prostate adenocarcinoma[20]. Conditional deletion of APC in the mouse prostate elevates nuclear β-catenin and results in prostatic adenocarcinoma formation[21]. Intriguingly, mutations in APC, β-catenin, and other components of the β-catenin destruction complex are rare in human PCa[22, 23], suggesting alternative mechanisms of β-catenin dysregulation in prostate tumorigenesis. One of such alternative mechanisms is the hypermethylation of the *APC* promoter region, which ultimately results in aberrant activation of β-catenin/Wnt signaling pathway. In fact, APC promoter hypermethelation in PCa has been correlated with poor clinical prognosis[24] and recently has been proposed as one of prognostic PCa markers[25].

Despite the elusiveness of aberrant Wnt activation, an interaction between the AR and β-catenin proteins has been identified in PCa cells[26–28]. A recent integrative genomic study revealed a significant enrichment of the androgen and Wnt signaling pathways in the early onset PCa samples but not in the elderly-onset PCa samples[29], which further implicates a clinical importance of both androgen and Wnt signaling in prostate tumorigenesis. However, the biological significance of this interaction in the pathogenesis of PCa remains unknown.

Author Manuscript Author Manuscript Author Manuscript Author Manuscript

To address this critical question and recapitulate the AR and β-catenin interaction *in vivo*, we developed *Ctnnb1$^{L(ex3)/+}$/R26hAR$^{L/+}$:PB-Cre4* mice, in which transgenic AR and stabilized β-catenin are co-expressed in prostatic epithelial cells. We observed accelerated tumor development, aggressive tumor invasion, and a decreased survival rate in these compound mice versus control littermates. Castration of these mice resulted in significant tumor regression. Moreover, implantation of prostatic epithelial cells isolated from the compound mice regenerated much severe PIN and prostatic adenocarcinoma lesions in tissue recombination assays. Furthermore, we detected increased expression of known pro-tumorigenic and pro-metastatic genes Spp1, Egr1, c-Myc, and Sp6 in the prostates of the compound mice. These data demonstrate a confounding role of androgen signaling in β-catenin-mediated oncogenic transformation in prostate tumorigenesis.

RESULTS

Activation of transgenic AR expression accelerates oncogenic transformation in the mouse prostate

Although an interaction between the androgen and Wnt signaling pathways has been identified in PCa cells, the significance of this interaction in prostate tumorigenesis remains unclear. Specifically, we still do not know whether these two pathways can synergistically promote PCa initiation and progression. To address this question, we developed *Ctnnb1$^{L(ex3)/+}$/R26hAR$^{L/+}$:PB-Cre4* mice, in which expression of human *AR* transgene and stabilized β-catenin were activated through the probasin promoter driven *Cre* expression in the mouse prostate (Fig. 1A). Using genomic PCR and Western blot analyses, we confirmed *LoxP/Cre* mediated recombination events (Fig. 1B), resulting in human AR and stabilized β-catenin protein expression in mouse prostate tissues (Fig. 1C). *Ctnnb1$^{L(ex3)/+}$/ R26hAR$^{L/+}$:PB-Cre4, Ctnnb1$^{L(ex3)/+}$:PB-Cre4, and R26hAR$^{L/+}$:PB-Cre4* mice were born at the expected Mendelian ratios and appeared normal with no obvious differences from their wild-type littermates at birth. We systematically examined male mice at 3, 4, 5, 6, and 8 weeks of age (Supplemental Figure 1, SFig. 1). Consistent with previous reports[30, 31], we did not observe any obvious abnormalities in 2 week to 12 month old *R26hAR$^{L/+}$:PB-Cre4* mice (data not shown). Adhering to recommendations of the Mouse Models of Human Cancers Consortium Prostate Pathology Committee[32], we first identified prostatic hyperplasia and mPIN1 in 4 week old *Ctnnb1$^{L(ex3)/+}$:PB-Cre4* mice (Fig. 1D1–3 and SFig. 1B1–2). These lesions originated predominantly in the dorsal/lateral prostate (D/LP) and ventral prostate (VP) lobes. Over time it appears that these low-grade mPIN lesions progressed towards high-grade mPIN lesions (mPIN3 and mPIN4) (SFig. 1D1–2 and 1E1–2). Notably, *Ctnnb1$^{L(ex3)/+}$/R26hAR$^{L/+}$:PB-Cre4* compound mice, with transgenic AR and stabilized β-catenin co-expression in the prostate, developed PIN lesions earlier than *Ctnnb1$^{L(ex3)/+}$:PB-Cre4* mice. We observed mPIN1 and mPIN2 lesions at 3-week-old age (SFig. 1A4), and mPIN3 and mPIN4 lesions at 5-weeks in *Ctnnb1$^{L(ex3)/+}$/R26hAR$^{L/+}$:PB-Cre4* mice (SFig. 1C3–4). Additionally, squamous metaplasia appeared in both *Ctnnb1$^{L(ex3)/+}$:PB-Cre4* and *Ctnnb1$^{L(ex3)/+}$/R26hAR$^{L/+}$:PB-Cre4* mice (SFig. 1C3, 1D2, 1D4 and 1E3). Expression of stabilized β-catenin was confirmed in prostatic epithelial cells in both *Ctnnb1$^{L(ex3)/+}$:PB-Cre4* and *Ctnnb1$^{L(ex3)/+}$/R26hAR$^{L/+}$:PB-Cre4* mice (Fig. 1D5 and 1E5, and SFig. 2A1–3 and 2C1–3). Interestingly, we noted atypical cell foci with stabilized

Author Manuscript Author Manuscript Author Manuscript Author Manuscript

β-catenin expression within PIN lesions of *Ctnnb1$^{L(ex3)/+}$:PB-Cre4* mice (arrows, Fig. 1D5, and SFig. 2A1 and 2A3). Transgenic AR expression was only detected in prostatic epithelial cells in *Ctnnb1$^{L(ex3)/+}$/R26hAR$^{L/+}$:PB-Cre4* compound mice (Fig. 1E6, and SFig. 2D1–3). To establish the nature of interaction between stabilized β-catenin with endogenous and transgenic AR, we performed co-immunoprecipitation experiments using whole cells lysates isolated from prostate tissues of 3-month-old *Ctnnb1$^{L(ex3)/+}$:PB-Cre4* and *Ctnnb1$^{L(ex3)/+}$/R26hAR$^{L/+}$:PB-Cre4* mice. As shown in Figure 1F, both endogenous and transgenic AR interact with stabilized and wild type β-catenin. The results further demonstrate the protein-protein interaction between stabilized β-catenin with both transgenic and endogenous AR, and implicate that a collaborative relationship between androgen and Wnt signaling pathways may synergistically promote the initiation of oncogenic transformation in the mouse prostate.

Co-expression of transgenic AR and stabilized β-catenin induces invasive prostate adenocarcinoma development

Following the consensus that high-grade mPIN lesions can progress to prostate adenocarcinomas, we continued examining both *Ctnnb1$^{L(ex3)/+}$:PB-Cre4* and *Ctnnb1$^{L(ex3)/+}$/R26hAR$^{L/+}$:PB-Cre4* mice for extended periods of time. We observed prostatic tumor formation in these mice beginning at 3 months of age. Gross examination revealed extensive prostatic tumor masses with multiple lobules in *Ctnnb1$^{L(ex3)/+}$/R26hAR$^{L/+}$:PB-Cre4* mice than those in age matched *Ctnnb1$^{L(ex3)/+}$:PB-Cre4* littermates (Fig. 2B1 versus 2A1, and 2B2 versus 2A2). Histologically, larger and more extensive prostatic tumor masses appeared in *Ctnnb1$^{L(ex3)/+}$/R26hAR$^{L/+}$:PB-Cre4* than in *Ctnnb1$^{L(ex3)/+}$/R26hAR$^{L/+}$:PB-Cre4* mice (Fig. 2D1 versus 2C1, and 2D2 versus 2C2). By 3 months of age *Ctnnb1$^{L(ex3)/+}$/R26hAR$^{L/+}$:PB-Cre4* developed multi-focal intracystic adenocarcinomas with extensive microinvasion in all prostatic lobes (Fig. 2D1, 2G, & 2G'). These lesions further progressed into invasive prostatic adenocarcinomas in 4 of 4 *Ctnnb1$^{L(ex3)/+}$/R26hAR$^{L/+}$:PB-Cre4* mice by 4 months of age (Fig. 2D2, 2H & 2H'). In contrast, *Ctnnb1$^{L(ex3)/+}$:PB-Cre4* mice showed milder changes, featuring high grade PINs and scattered intracystic adenocarcinomas at 3 months (Fig. 2C1, 2E & 2E') and more frequent intracystic andenocarcinomas with rare microinvasion at 4 months (Fig. 2C2, 2F & 2F'). These data demonstrate that *Ctnnb1$^{L(ex3)/+}$/R26hAR$^{L/+}$:PB-Cre4* mice have accelerated tumor growth compared to *Ctnnb1$^{L(ex3)/+}$:PB-Cre4* mice, suggesting a synergistic effect of stabilized β-catenin and transgenic AR co-expression in enhancing oncogenesis and accelerating invasive prostatic adenocarcinoma formation.

Ctnnb1$^{L(ex3)/+}$/R26hAR$^{L/+}$:PB-Cre4 compound mice showed a shortened survival rate

Systematic analysis showed that *Ctnnb1$^{L(ex3)/+}$/R26hAR$^{L/+}$:PB-Cre4* mice have a significantly earlier onset and faster progressing tumor phenotype than *R26hAR$^{L/+}$:PB-Cre4* and *Ctnnb1$^{L(ex3)/+}$:PB-Cre4* mice (Fig. 2I). Three of three *Ctnnb1$^{L(ex3)/+}$/R26hAR$^{L/+}$:PB-Cre4* mice developed multifocal intracystic adenocarcinomas with microinvasive lesions as early as at 2 months of age. At 4 months of age, 4 of 4 *Ctnnb1$^{L(ex3)/+}$/R26hAR$^{L/+}$:PB-Cre4* mice showed massive intracystic adenocarcinomas with extensive invasion in multiple prostatic lobes. *Ctnnb1$^{L(ex3)/+}$/R26hAR$^{L/+}$:PB-Cre4* mice die spontaneously between 6 to 9 months, which is significant shorter than *Ctnnb1$^{L(ex3)/+}$:PB-Cre4* and *R26hAR$^{L/+}$:PB-Cre4*

Author Manuscript Author Manuscript Author Manuscript Author Manuscript

littermates (Fig. 3A). The average weight of prostate tumor tissues at 7 months in *Ctnnb1*$^{L(ex3)/+}$*/R26hAR*$^{L/+}$*:PB-Cre4* mice was significant heavier than those of age matched *R26hAR*$^{L/+}$*:PB-Cre4*, and *Ctnnb1*$^{L(ex3)/+}$*:PB-Cre4* littermates (Fig. 3B). Based on systematic gross and histologic examination by a board-certified veterinary pathologist, prostatic tumor burden was the most likely cause of death for all of these mice. Shorter survival rate in *Ctnnb1*$^{L(ex3)/+}$*/R26hAR*$^{L/+}$*:PB-Cre4* mice, as compared to controls, further demonstrate that *Ctnnb1*$^{L(ex3)/+}$*/R26hAR*$^{L/+}$*:PB-Cre4* mice have accelerated prostate tumor development and more aggressive tumor phenotype.

Transgenic AR and stabilized β-catenin co-expression synergistically enhances cell proliferation

In this study, we examined the effect of co-expressing stabilized β-catenin and transgenic AR in promoting cell proliferation in the transgenic mice using Ki67 immunohistochemistry. A significant increase of Ki67 positive cells was observed in the samples of *Ctnnb1*$^{L(ex3)/+}$*/R26hAR*$^{L/+}$*:PB-Cre4* versus *Ctnnb1*$^{L(ex3)/+}$*:PB-Cre4* mice (Fig. 3C1–E2). We quantified Ki67 positive cells per 1000 epithelial cells from five fields on three different slides that were prepared independently from three mice of each genotype. As shown in Figure 3F, the epithelial proliferative index was the highest in the tumor lesions of *Ctnnb1*$^{L(ex3)/+}$*/R26hAR*$^{L/+}$*:PB-Cre4* mice, suggesting a synergistic role of transgenic AR and stabilized β-catenin co-expression in promoting cell proliferation in the mouse prostate.

Transgenic AR and stabilized β-catenin co-expression induces oncogenic transformation predominantly in prostatic luminal cells

To further define the cellular properties of prostatic pathologies developed in *Ctnnb1*$^{L(ex3)/+}$*:PB-Cre4, and Ctnnb1*$^{L(ex3)/+}$*:R26hAR*$^{L/+}$*:PB-Cre4* mice, we comprehensively analyzed different cellular markers in both higher-grade PIN and adenocarcinoma lesions (Fig. 4). Most atypical and tumor cells showed positive immunoreactivity for E-cadherin (Fig. 4D1–4) and CK8 (Fig. 4E1–4), secretory epithelial markers, but showed no immunoreactivity for the neuroendocrine cell marker synaptophysin (Fig. 4H1–4). Immunoreactivity for p63, a cellular marker for prostatic basal epithelial cells, appeared mainly in the basal compartment of prostatic glands with PIN lesions, but was lacking in tumor lesions of both *Ctnnb1*$^{L(ex3)/+}$*:PB-Cre4* and *Ctnnb1*$^{L(ex3)/+}$*/R26hAR*$^{L/+}$*:PB-Cre4* mice (Fig. 4G1–4). CK5 antibodies demonstrated similar staining patterns as those of p63 (Fig. 4F1–4). Positive cytoplasmic and nuclear reactivity with β-catenin antibodies appeared in both PIN and tumor sections isolated from *Ctnnb1*$^{L(ex3)/+}$*:PB-Cre4* and *Ctnnb1*$^{L(ex3)/+}$*/R26hAR*$^{L/+}$*:PB-Cre4* mice (Fig. 4C1–4). In contrast, positive reactivity with the human AR antibody was only observed in PIN and tumor lesions of *Ctnnb1*$^{L(ex3)/+}$*/R26hAR*$^{L/+}$*:PB-Cre4* mice (Fig. 4B2 & B4). Taken together, these data imply that most atypical and tumor cells in both *Ctnnb1*$^{L(ex3)/+}$*:PB-Cre4* and *Ctnnb1*$^{L(ex3)/+}$*/R26hAR*$^{L/+}$*:PB-Cre4* mice contain prostatic luminal cellular markers.

Effect of abnormal activation of AR and β-catenin in inducing prostatic oncogenesis in tissue recombinants

In this study, we assessed the oncogenic potential of transgenic AR and stabilized β-catenin expressing cells to regenerate cancerous cells using a tissue recombination system. In the

Author Manuscript Author Manuscript Author Manuscript Author Manuscript

double-fluorescent mT/mG Cre reporter mouse strain, expression of membrane targeted tandem dimer Tomato (mT) or membrane-targeted green fluorescent protein (mG) is controlled by *Cre*-mediated recombination, where *Cre* expressing cells contain mG and can be sorted from mT cells[33]. We first generated and analyzed specific mG protein expression in prostatic luminal epithelial cells controlled by *PB-Cre* mediated recombination, allowing for the selection of recombined cells, in *mT/mG:PB-Cre* mice (SFig. 3). We then produced both *mT/mG/Ctnnb1*$^{L(ex3)/+}$*:PB-Cre4* and *mT/mG/ Ctnnb1*$^{L(ex3)/+}$*/R26hAR*$^{L/+}$*:PB-Cre4* mice to specifically label stabilized β-catenin only or stabilized β-catenin/transgenic AR positive cells (Fig. 5A and B). Single cell suspensions prepared from prostate tumors of 3-month-old *mT/mG/Ctnnb1*$^{L(ex3)/+}$*:PB-Cre4* or *mT/mG/Ctnnb1*$^{L(ex3)/+}$*/R26hAR*$^{L/+}$*:PB-Cre4* mice mixed with embryonic UGSM cells were transplanted under the renal capsule of NOD/SCID mice and analyzed after 12 weeks. Grafts composed solely of UGSM cells appeared small and fibrous and mainly contained stromal-like cells. However, large translucent grafts were observed in grafts containing both UGSM and prostatic epithelial cells. Histological analysis of these grafts showed tubular epithelial structures with prostatic-like ducts filled with fluid (Fig. 5C and 5D). We observed typical high-grade PIN or multi-focal intracystic adenocarcinoma lesions in tissue recombinant grafts prepared with prostatic epithelial cells isolated from mT/mG/*Ctnnb1*$^{L(ex3)/+}$*:PB-Cre4* or *mT/mG/Ctnnb1*$^{L(ex3)/+}$*/R26hAR*$^{L/+}$*:PB-Cre4* mice (arrows, Fig. 5C or 5D, and 5C' and 5D'). These were very similar to the lesions presenting in the prostates of *Ctnnb1*$^{L(ex3)/+}$*:PB-Cre4 and Ctnnb1*$^{L(ex3)/+}$*/R26hAR*$^{L/+}$*:PB-Cre4* mice. Of note were the more severe pathologic changes in grafts using prostatic epithelial cells isolated from mT/mG/*Ctnnb1*$^{L(ex3)/+}$*/R26hAR*$^{L/+}$*:PB-Cre4* versus mT/mG/*Ctnnb1*$^{L(ex3)/+}$*:PB-Cre4* mice. Co-expression of transgenic AR and/or stabilized β-catenin, as well as mG protein, was detected in atypical and tumor cells of all graft samples (Fig. 5E–P). These data further demonstrate the oncogenic capacity of transgenic AR and stabilized β-catenin in regenerating cancerous glandular structures in the mouse prostate.

Androgen signaling is a confounding factor for β-catenin initiated oncogenic transformation

Early onset and rapidly progressing tumor phenotype in *Ctnnb1*$^{L(ex3)/+}$*/R26hAR*$^{L/+}$*:PB-Cre4* compound mice suggests a promotional role of androgen signaling in β-catenin mediated oncogenic transformation. Thus, we evaluated the effect of castration on tumor development, maintenance, and progression in the transgenic mice. Given the fact that PINs developed as early as 3 weeks in *Ctnnb1*$^{L(ex3)/+}$*/R26hAR*$^{L/+}$*:PB-Cre4* mice, we castrated *R26hAR*$^{L/+}$*:PB-Cre4, Ctnnb1*$^{L(ex3)/+}$*:PB-Cre4* and *Ctnnb1*$^{L(ex3)/+}$*/R26hAR*$^{L/+}$*:PB-Cre4* mice at 2 weeks of age and analyzed them at 16 weeks of age to determine the effect of androgens in initiating oncogenic transformation in the prostate (Fig. 6A). We observed underdeveloped prostate lobes in all three different genotypes of mice, featuring markedly atrophic glandular/ductal profiles in combination with a relatively prominent concentric peri-glandular/-ductular fibromuscular stroma (Fig. 6B–D'). Importantly, there were no proliferative, dysplasic and mPIN pathological changes in *Ctnnb1*$^{L(ex3)/+}$*:PB-Cre4* nor *Ctnnb1*$^{L(ex3)/+}$*/R26hAR*$^{L/+}$*:PB-Cre4* mice, contrasting to those age- and genotype-matched intact mice (Fig. 1), which implicates an essential role of androgens in initiating oncogenic transformation of the prostate. To assess androgens in promoting tumor growth and progression, we castrated *Ctnnb1*$^{L(ex3)/+}$*:PB-Cre4* and *Ctnnb1*$^{L(ex3)/+}$*/R26hAR*$^{L/+}$*:PB-Cre4* mice at 6 weeks, after

Author Manuscript Author Manuscript Author Manuscript Author Manuscript

high-grade PINs have already developed, and then analyzed them at 16 weeks (Fig. 6A). Prostate lobes were grossly smaller than the age matched intact mice and histologic analysis showed some residual mPIN-like lesions as well as remnants of sloughed, intraluminal keratin. However, the epithelial cells lining these mPIN-like lesions consisted of 1 to 2 cell layers of uniform cuboidal cells with minimal nuclear atypia (Fig. 6E–H'). Extensive peri- and inter- glandular/ductular inflammatory responses appeared in both castrated *Ctnnb1$^{L(ex3)/+}$:PB-Cre4*, and *Ctnnb1$^{L(ex3)/+}$/R26hAR$^{L/+}$:PB-Cre4* mice. We continued the study by castrating *Ctnnb1$^{L(ex3)/+}$:PB-Cre4* and *Ctnnb1$^{L(ex3)/+}$/R26hAR$^{L/+}$:PB-Cre4* at 16 weeks when they developed prostatic adenocarcinomas. At 26 weeks of age, we observed regression of tumor masses in all prostate lobes (Fig. 6A). Although residual lower grade mPIN lesions still remained, no tumor masses were observed in all examined samples isolated from *Ctnnb1$^{L(ex3)/+}$/R26hAR$^{L/+}$:PB-Cre4* mice castrated at 16 weeks (Fig. 6I–L'). We also detected massive cell death in all prostatic lobes, accompanied with extensive immune responses. To further explore the effect of androgens on tumor growth in *Ctnnb1$^{L(ex3)/+}$:PB-Cre4* and *Ctnnb1$^{L(ex3)/+}$/R26hAR$^{L/+}$:PB-Cre4* mice, we supplemented androgen pellets into the mice that were castrated at 16 weeks of age (SFig. 5A). Importantly, we observed that more severe PIN lesions re-developed in castrated *Ctnnb1$^{L(ex3)/+}$/R26hAR$^{L/+}$:PB-Cre4* than *Ctnnb1$^{L(ex3)/+}$:PB-Cre4* mice at 30 weeks of age, 4 weeks after androgen pellet supplement (SFig. 5E versus 5B). Transgenic hAR expression was only detected in the prostates of *Ctnnb1$^{L(ex3)/+}$/R26hAR$^{L/+}$:PB-Cre4* mice (SFig. 5F and 5F'), but not in ones of *Ctnnb1$^{L(ex3)/+}$:PB-Cre4* mice (SFig. 5C and 5C'). Stabilized β-catenin was observed in the prostates of both *Ctnnb1$^{L(ex3)/+}$:PB-Cre4* and *Ctnnb1$^{L(ex3)/+}$/R26hAR$^{L/+}$:PB-Cre4* mice, respectively (SFig. 5D to 5G'). These experiments further demonstrate a reliance on androgens in β-catenin-mediated oncogenic transformation in the mouse prostate.

Identification of downstream targets that promote prostate tumor initiation and progression

Next, we performed microarray analyses to investigate the molecular basis by which transgenic AR and stabilized β-catenin expression may promote prostate tumorigenesis in these transgenic mice. We carefully isolated prostatic tumor tissues from 4-month-old *Ctnnb1$^{L(ex3)/+}$:PB-Cre4* and *Ctnnb1$^{L(ex3)/+}$/R26hAR$^{L/+}$:PB-Cre4* mice and microscopically confirmed that the tumor tissues used to prepare RNA samples for microarray studies were composed of more than 80 % tumor cells. Analyses of gene-expression profiles yielded differential expression of more than 8 fold in 625 genes in samples from *Ctnnb1$^{L(ex3)/+}$/R26hAR$^{L/+}$:PB-Cre4* and *Ctnnb1$^{L(ex3)/+}$:PB-Cre4* mice in comparison to those from age and sex-matched *R26hAR$^{L/+}$:PB-Cre4* mice, reflecting that the change in expression of these genes resulted from stabilized β-catenin expression. The top 100 up- and down-regulated genes are shown in SFig. 6. With real-time quantitative RT-PCR (qPCR), we confirmed an up-regulation of Spp1, Egr1, Bex1, Sp6, Lef1, Axin2, Cd44, and c-Myc among those genes (Fig. 7A to 7C). Of note, expression of Spp1, Egr1, Bex1, c-Myc and Sp6 transcripts in prostate tissues isolated from *Ctnnb1$^{L(ex3)/+}$/R26hAR$^{L/+}$:PB-Cre4* mice was significantly higher than those from *Ctnnb1$^{L(ex3)/+}$:PB-Cre4* or *R26hAR$^{L/+}$:PB-Cre4* mice (Fig. 7B and 7C), implying the need for both transgenic AR and stabilized β-catenin expression in regulating transcription of these genes. Intriguingly, previous studies have implicated the

Author Manuscript Author Manuscript Author Manuscript Author Manuscript

promotional roles of these gene products in PCa initiation and progression[34–36]. Using immunohistochemistry, we demonstrated an increased expression of Spp1 and Egr-1 proteins in the prostates of *Ctnnb1*$^{L(ex3)/+}$*/R26hAR*$^{L/+}$*:PB-Cre4* mice (Fig. 7D). Expression levels of *Lef1, Axin2*, and *Cd44*, which have been documented as β-catenin downstream targets, were higher in the samples isolated from *Ctnnb1*$^{L(ex3)/+}$*:PB-Cre4* mice than those from *Ctnnb1*$^{L(ex3)/+}$*/R26hAR*$^{L/+}$*:PB-Cre4* mice (Fig. 7C). Additionally, to further explore the possible molecular basis for stabilized β-catenin and transgenic AR in regulating gene expression, we performed ChIP assay with prostatic cells isolated from 3-months-old *Ctnnb1*$^{L(ex3)/+}$*:PB-Cre4* and *Ctnnb1*$^{L(ex3)/+}$*/R26hAR*$^{L/+}$*:PB-Cre4* mice. We analyzed the mouse c-Myc locus, one of the up-regulated genes in prostate tissues isolated from *Ctnnb1*$^{L(ex3)/+}$*/R26hAR*$^{L/+}$*:PB-Cre4* mice with the immuno-precipitated genomic DNA by qPCR using specific primers spanning the mouse c-Myc locus (Fig. 7E)[37]. We observed the recruitment of both AR and β-catenin at β-catenin/TCF4-binding regions on the mouse c-Myc locus (Fig. 7F). Interestingly, the enrichments of β-catenin and AR at β-catenin/TCF4-binding regions were higher in the samples isolated from *Ctnnb1*$^{L(ex3)/+}$*/R26hAR*$^{L/+}$*:PB-Cre4* mice than ones from *Ctnnb1*$^{L(ex3)/+}$*:PB-Cre4* mice. Overall, the data indicate that co-activation of transgenic AR and β-catenin expression regulates the transcription of a unique subset of genes, which may contribute to prostate tumor initiation and progression.

DISCUSSION

It has been over a decade since the interaction between AR and β-catenin has been demonstrated in PCa cells[26–28, 38]. However, the biological consequences of this interaction in prostate tumorigenesis remain unclear. In this study, we directly addressed this long-term unclear question using a series of newly developed mouse models. We observed accelerated invasive tumor development and a shortened survival in *Ctnnb1*$^{L(ex3)/+}$*/R26hAR*$^{L/+}$*:PB-Cre4* mice, in which the expression of both transgenic AR and stabilized β-catenin proteins is concurrent in prostate epithelial cells. In contrast, *Ctnnb1*$^{L(ex3)/+}$*:PB-Cre4* mice, which only have stabilized β-catenin expression in the prostate, displayed a milder tumor phenotype. Because endogenous AR expression exists in prostatic luminal cells of *Ctnnb1*$^{L(ex3)/+}$*:PB-Cre4* mice and castration prior to puberty did not result in tumor development, our observation implies an essential role for androgen signaling in enhancing β-catenin mediated prostate tumor initiation. Importantly, a recent study has shown an enrichment of AR and Wnt signaling pathways in early-onset PCa, but not in elderly-onset PCa[29], highlighting a clinical significance for this study. As mutations in APC, β-catenin, and other components of the β-catenin destruction complex have rarely been detected in PCa cells, results from this current study suggest a possible mechanism underlying abnormal activation of Wnt/β-catenin signaling in prostate tumorigenesis. As more than 100 AR co-regulators have been identified[39], with their roles in prostate tumorigenesis remaining largely uncharacterized, this study provides a novel model that recapitulates the biological roles of AR and β-catenin, its co-regulator, during the course of PCa initiation and progression *in vivo*.

To determine the extent of the role that androgens play in prostate tumorigenesis, we pursued a series of castration experiments in this study. When mice were castrated at two weeks, prostate gland development was impaired in all mice with different genotypes and no PIN or other malignant lesions was observed in both *Ctnnb1*$^{L(ex3)/+}$*/R26hAR*$^{L/+}$*:PB-Cre4*

Author Manuscript Author Manuscript Author Manuscript Author Manuscript

and *Ctnnb1*$^{L(ex3)/+}$*:PB-Cre4* mice at 16 weeks of age, indicating an essential role of androgens in β-catenin-mediated oncogenic transformation. To further examine the effect of androgens on maintenance and progression of prostate tumors, we analyzed both *Ctnnb1*$^{L(ex3)/+}$*/R26hAR*$^{L/+}$*:PB-Cre4* and *Ctnnb1*$^{L(ex3)/+}$*:PB-Cre4* mice that were castrated at 6 or 16 weeks of age, when PINs or prostate adenocarcinomas had already developed (Fig. 6A). We observed significant regression of PIN and prostatic adenocarcinomas in both *Ctnnb1*$^{L(ex3)/+}$*/R26hAR*$^{L/+}$*:PB-Cre4* and *Ctnnb1*$^{L(ex3)/+}$*:PB-Cre4* mice. Importantly, when androgen pellets were implanted into castrated mice, we observed a re-growth of transgenic AR and stabilized β-catenin positive prostate tumor cells (SFig. 5). Histological analyses of those prostate tissues showed more severe pathological changes in the prostate tissues isolated from *Ctnnb1*$^{L(ex3)/+}$*/R26hAR*$^{L/+}$*:PB-Cre4* than *Ctnnb1*$^{L(ex3)/+}$*:PB-Cre4* mice. These data highlight the importance of androgen signaling in maintaining and promoting β-catenin-mediated prostatic tumor formation and progression, and also correlate these mouse models with human early-onset PCa, which are thought to have a unique AR signature[29]. These features that mimic some unique aspects of early-onset PCa may also enable further study of these pathways potentially resulting in more target therapy development for PCa.

We observed either high-grade PIN or prostatic adenocarcinoma lesions in regenerated samples using epithelial cell suspensions isolated from *Ctnnb1*$^{L(ex3)/+}$*:PB-Cre4* or *Ctnnb1*$^{L(ex3)/+}$*/R26hAR*$^{L/+}$*:PB-Cre4* mice, respectively. Because prostatic cells with transgenic AR and stabilized β-catenin expression were also labeled with GFP expression, we confirmed that the regenerated PIN and adenocarcinoma lesions were derived solely from transgenic AR and stabilized β-catenin expressing epithelial cells. In this set of experiments, regenerated PIN and cancerous lesions were very similar to the malignant changes that appeared in the prostates of *Ctnnb1*$^{L(ex3)/+}$*:PB-Cre4* or *Ctnnb1*$^{L(ex3)/+}$*/R26hAR*$^{L/+}$*:PB-Cre4* mice. The cell suspensions isolated from *Ctnnb1*$^{L(ex3)/+}$*/R26hAR*$^{L/+}$*:PB-Cre4* developed prostatic adenocarcinomas, whereas suspensions from *Ctnnb1*$^{L(ex3)/+}$*:PB-Cre4* mice only produced high-grade PIN lesions. This result further demonstrates a synergistic effect of co-expression of transgenic AR and stabilized β-catenin in promoting oncogenic transformation in prostate cells. In this study, we also directly implanted mouse PCa tissues in the grafting assays[40] and observed the similar results (SFig. 4).

Using microarray approaches, we searched for the molecular targets that are responsible for PIN and prostatic adenocarcinoma development. We observed higher expression of several β-catenin downstream targets, including Lef1, Axin2, and Cd44 in the prostatic tissues of *Ctnnb1*$^{L(ex3)/+}$*:PB-Cre4* compared to those from *Ctnnb1*$^{L(ex3)/+}$*/R26hAR*$^{L/+}$*:PB-Cre4* and *R26hAR*$^{L/+}$*:PB-Cre4* mice. We also observed a subset of pro-tumorigenic and pro-metastatic genes that show higher expression levels in prostate tissues of *Ctnnb1*$^{L(ex3)/+}$*/R26hAR*$^{L/+}$*:PB-Cre4* compound mice, including Spp1, Egr-1, Bex1, c-Myc, and Sp6. *SPP1* is a pro-metastasis invasion gene identified in human PCa that has been suggested as a prognostic marker for disease recurrence and lethal metastasis[34]. Increased Spp1 expression has been shown to contribute to the metastatic phenotype in both *in vitro* and *in vivo* studies. EGR-1 (early growth response-1) was upregulated in human prostate tumors and related to tumor progression[35]. Interestingly, Bex1 and Sp6 have also been implicated in breast cancer therapy resistance and linked to the regulation of Wnt-BMP signaling pathway[41, 42].

Author Manuscript Author Manuscript Author Manuscript Author Manuscript

Because both AR and β-catenin are transcriptional regulators, we assessed their collaborative role in regulating transcription using our mouse models. We detected the recruitment of both AR and β-catenin on the endogenous mouse *c-Myc* promoter region. Intriguingly, the intensity of PCR fragments containing the β-catenin binding regions was higher in the samples of *Ctnnb1*$^{L(ex3)/+}$*/R26hAR*$^{L/+}$*:PB-Cre4* mice than ones of *Ctnnb1*$^{L(ex3)/+}$*:PB-Cre4* mice, suggesting that co-recruitment of the AR and β-catenin on the c-Myc promoter increases transcription activity in PCa cells of *Ctnnb1*$^{L(ex3)/+}$*/R26hAR*$^{L/+}$*:PB-Cre4* mice. Currently, we are pursuing more mechanistic in-depth experiments to investigate the collaborative regulation of AR and β-catenin in distinct gene expression.

Lastly, we observed that the most atypical and tumor cells in PIN and adenocarcinoma lesions of both *Ctnnb1*$^{L(ex3)/+}$*:PB-Cre4* and *Ctnnb1*$^{L(ex3)/+}$*/R26hAR*$^{L/+}$*:PB-Cre4* mice were E-cadherin and CK8 positive, but synaptophysin negative, suggesting that oncogenic transformation may be initiated in luminal epithelial cells. It has been shown that prostatic luminal epithelial cells are AR positive and can function as tumor initiating cells[43, 44], a feature of the tumor cells that we confirmed in our regeneration assays. Given the evidence that the probasin promoter is primarily active in prostatic luminal cells, our current data suggest that the dysregulation of androgen and β-catenin signaling pathways results in prostatic oncogenic transformation predominately in luminal epithelial cells. Furthermore, as demonstrated in this study, identification of a synergistic effect of AR and β-catenin on PCa development and progression suggests a novel mechanism for dysregulation of AR and β-catenin expression that is different from that of single gene, AR or β-catenin, alterations that potentially recapitulates features observed in early-onset PCa tumorigenesis. Therefore, more in-depth investigations using these newly developed mouse models should further enhance our knowledge regarding androgen and Wnt signaling pathways in prostate tumorigenesis.

MATERIALS AND METHODS

Mouse Breeding, Genotyping and Castration

All animal experiments performed in this study were approved by the Administrative Panel on Laboratory Animal Care at Stanford University. All mice were used in this study were on a C57BL/6 background. Mice containing the conditional *Ctnnb1* allele (*Ctnnb1*$^{lox(ex3)}$) were obtained from Dr. Makoto M. Taketo[45]. *R26hAR*$^{loxP/wt}$*:PB-Cre4* mice were generated by crossing between *R26hAR*$^{loxP/wt}$[31] and *PB-Cre4* mice[46]. *Ctnnb1*$^{lox(ex3)/lox(ex3)}$ female mice were intercrossed with *R26hAR*$^{loxP/wt}$*:PB-Cre4* males to generate *Ctnnb1*$^{L(ex3)/+}$*/ R26hAR*$^{L/+}$*:PB-Cre4* and *Ctnnb1*$^{L(ex3)/+}$*:PB-Cre4* littermates. Mice were genotyped by PCR as described previously[31, 47, 48]. The forward primer, 5’-TCCTCAGAGAGCCTCGGCTAGGTAG-3’, was used with the reverse primer, 5’-CCGTAAGTTATGTAACGCGGAACTC-3’, or 5’-TCTGTCTAGGGGTTGGATAAGCCAG-3’, to detect the AR target or wild type allele[31], respectively. The *Ctnnb1* conditional and wild type alleles were detected with the forward, 5’-AACTGGCTTTTGGTGTCGGG-3’, and reverse primers, 5’-TCGGTGGCTTGCTGATTATTTC-3’[45]. The forward primer, 5’-TTGCCTGCATTACCGGTCGATGCA-3’, and the reverse primer, 5’-

Author Manuscript Author Manuscript Author Manuscript Author Manuscript

GATCCTGGCAATTTCGGCTAT-3', were used to detect the *Cre* transgene. Genomic DNA fragments were amplified at 95°C for 3 min, then 95°C for 45 sec, 58°C for 40 sec, and 72°C for 60 sec for 35 cycles, then 72°C for 5 min.

For castration, the mice were anesthetized by IP injection of Ketamine and Xylazine. Both testicles and epididymis were removed through a scrotal approach. The distal end of the spermatic cord was ligated with silk thread as described previously[49]. For androgen treatment, testosterone pellets (12.5 mg, Innovative Research of America) were placed in castrated mice subcutaneously to restore serum testosterone level.

In vivo Prostate Regeneration Assays

We obtained the double-fluorescent mT/mG:Cre reporter strain from Dr. Liqun Luo[33], and used it to generate *mT/mG/Ctnnb1*$^{L(ex3)/+}$*/R26hAR*$^{L/+}$*:PB-Cre4* and m*T/mG/Ctnnb1*$^{L(ex3)/+}$*:PB-Cre4* mice. Prostate tissues from the above mice were minced into small pieces of one cubic millimeter, digested in DMEM/Collagenase/FBS for 3 hours at 37°C, and 0.25% Trypsin-EDTA (Invitrogen, Carlsbad, CA) on ice for 1 hour. Digested cells were pipetted vigorously to dissociate cell clumps and then passed through 70 μm cell strainers (BD Biosciences, San Jose, CA) to obtain single-cell suspensions. Mouse urogenital sinus mesenchymal (UGSM) cells were prepared as described previously[50]. UGSM cells were cultured in DMEM/5% FBS/5% Nu-serum/5μg/ml insulin/10^{-8} M 5α-dihydrotestosterone. Approximately 1×10^5 of prostatic epithelial and UGSM cells were mixed and resuspended in transplantation solution, 1:1 (v/v) PBS:Matrigel (BD Biosciences, San Jose, CA), and transplanted under the renal capsule of 6 to 8-week-old male NOD/SCID mice.

Histological analyses and immunohistochemistry

In this study, we used the new guidelines recommended by The Mouse Models of Human Cancers Consortium Prostate Pathology Committee in 2013 for our pathological analyses[32]. Mouse tissues were fixed and processed as described in our previous study[31]. Tissue slides were exposed to different first antibodies in PBS with 1% goat serum at 4°C overnight, including 1:500 dilution of anti-human AR (sc-7305, Santa Cruz), 1:500 dilution of anti-mouse/human AR (sc-816, Santa Cruz), 1:250 dilution of anti-p63 (sc-8431, Santa Cruz), 1:3000 dilution of anti Ki67 (NCL-ki67, Novacastra), 1:500 dilution of anti-β-catenin (sc-7199, Santa Cruz), 1:300 dilution of anti-E-cadherin (c20820, Transduction Laboratories), 1:800 dilution of anti-CK5 (PRB-160P, Covance), 1:800 dilution of anti-CK8 (MMS-162P, Covance), 1:200 dilution of anti-synaptophysin (18-0130, Invitrogen), 1:100 dilution of anti-SPP1 (91655, Abcam), and 1:50 dilution of anti-Egr1 (4153, Cell Signaling) antibodies. Slides were then incubated with biotinylated anti-rabbit or anti-mouse secondary antibody (BA-1000 or BA-9200, Vector Laboratories) for 1 h, horseradish peroxidase streptavidin (SA-5004, Vector Laboratories) for 30 min, and then visualized by DAB kit (SK-4100, Vector Laboratories). All samples were subsequently counterstained with 5% (w/v) Harris Hematoxylin.

RNA Isolation and Reverse Transcription (RT)-Quantitative PCR (qPCR) Assays

Mouse prostate tissues were homogenized in RNA-Bee (TEL-TEST, Inc., Friendswood, TX) and total RNA was isolated as recommended by the manufacturer. Reverse transcription was

Author Manuscript Author Manuscript Author Manuscript Author Manuscript

carried out following our previous report[51]. For quantitative PCR, cDNA samples were mixed with SYBR GreenER qPCR Super Mix Universal (11762, Invitrogen) and specific primers in the MX 3005P thermocycler (Stratagene), and performed quantitative PCR according to the manufacturer's protocol. Relative mRNA levels were calculated by Delta Delta C(T) method[52]. Reactions were done in triplicate and the values were normalized by GAPDH expression levels. Primers for Spp1 (5-ATCTCACCATTCGGATGAGTCT-3; 5-TGTAGGGACGATTGGAGTGAAA-3), Egr1 (5-TCGGCTCCTTTCCTCACTCA-3; 5-CTCATAGGGTTGTTCGCTCGG-3), Sp5 (5-TGGGTTCACCCTCCAGACTTT-3; 5-CCGGCGAGAACTCGTAAGG-3), Sp6 (5-CCTGCAACCTCTCCAGACATA-3; 5-GCCCTGTGAAAAGTCTACCTCC-3), Bex1 (5-ATGGAGTCCAAAGATCAAGGCG-3; 5-CTGGCTCCCTTCTGATGGTA-3), Ect2 (5-TTGGGCCACCAGTTATACTCA-3; 5-CCAGGTTCAGCATACTCGTACAA-3), Lef1 (5-TGTTTATCCCATCACGGGTGG-3; 5-CATGGAAGTGTCGCCTGACAG-3), c-Myc (5-CCCTATTTCATCTGCGACGAG-3; 5-GAGAAGGACGTAGCGACCG-3), Axin2 (5-ATGAGTAGCGCCGTGTTAGTG-3; 5-GGGCATAGGTTTGGTGGACT-3), Cd44 (5-TCGATTTGAATGTAACCTGCCG-3; 5-CAGTCCGGGAGATACTGTAGC-3), and Gapdh (5-AGGTCGGTGTGAACGGATTTG-3; 5-TGTAGACCATGTAGTTGAGGTCA-3) were synthesized and used in the qPCR reactions, respectively.

Gene Expression Microarray and Analysis

RNA samples were isolated from age-matched mice of different genotypes. Fluorescently-labeled cDNA probes were prepared from extracted RNA samples and hybridized to Affymetrix Mouse Gene ST 2.0 arrays. Array hybridization, washing, and scanning were carried out per the manufacturer's instructions. Data processing and analysis were performed with Affymetrix Expression and Transcriptome Analysis Console software.

Co-immunoprecipitaion and Western Blotting

Mouse prostate tissues were isolated and processed as described previously[31, 47, 48]. Whole cell lysates were precleared for 20 min with 10 μl of protein-A/G-agarose beads (Pierce), and then incubated with pre-equilibrated protein-A/G-agarose beads with AR (sc-816, Santa Cruz) or β-catenin antibody (610154, BD bioscience) at 4 °C for 3 h. The beads were washed three times in lysis buffer and eluted by boiling in SDS-PAGE sample buffer. After SDS-PAGE, proteins were transferred to nitrocellulose (Schleicher & Schüll) and blocked in TBS-T (50 mM Tris-HCl, 150 mM NaCl, and 0.08% Tween 20) with 5% dry nonfat milk. Membranes were probed with β-catenin (610154, BD bioscience), human AR (sc-7305, Santa Cruz), or tubulin (MS-581, Lab Vision) antibody. Anti-rabbit or mouse IgG conjugated to horseradish peroxidase were used as secondary antibodies (Promega). Detection was performed with ECL reagents (Amersham Biosciences).

Chromatin immunoprecipitation (ChIP) Assays

ChIP assays were performed as described previously[53] In brief, single cell suspensions of prostatic cells isolated from 3-month-old *Ctnnb1*$^{L(ex3)/+}$*:PB-Cre* and *Ctnnb1*$^{L(ex3)/+}$*/R26hAR*$^{L/+}$*:PB-Cre* mice were incubated with 1% formaldehyde at room temperature. The cross-linking was quenched with 0.1 M glycine for 5 min. The cells washed sequentially with cold PBS, wash buffer I (0.25% Triton X-100, 10 mM EDTA, 0.5 mM EGTA, and 10

Author Manuscript Author Manuscript Author Manuscript Author Manuscript

mM HEPES at pH 6.5), and wash buffer II (200 mM NaCl, 1 mM EDTA, 0.5 mM EGTA, and 10 mM HEPES at pH 6.5). Cells were then lysed in lysis buffer (1% SDS, 10 mM EDTA, 50 mM Tris (pH 8.1). The chromatin was sheared to an average size of 500 bp by sonication, diluted 10-fold in ChIP dilution buffer (2 mM EDTA, 150 mM NaCl, 20 mM Tris-HCl (pH 8.1), and 1% Triton X-100), subjected to immunoprecipitation with either AR (sc-816, Santa Cruz) or β-catenin antibody (610254, BD Biosciences) overnight at 4 °C, and recovered with protein-A/G-agarose beads (Pierce). The immunoprecipitates were serially washed with different TSE (Triton/SDS/EDTA)-based buffers, and eluted for PCR analysis. The immuno-complexes were eluted from the beads through incubation with 10× bead volume of elution buffer (1% SDS and 0.1 M $NaHCO_3$). Cross-links were reversed by incubating the elution samples at 65 °C for 6 h, and chromatin DNA fragments were purified with a PCR purification kit (Qiagen). The above samples and inputs were analyzed by real-time qPCR using specific primers for the β-catenin/TCF4-binding regions on mouse c-Myc locus[37]; Primers for amplicon “A”, 5’-ACTCATTCGTTCGTCCTTC-3’ and 5’-CCTCGCTCCACACAATAC-3’, and for amplicon “B”, 5’-CTCACTGGAACTTACAATCTG-3’ and 5’-CAACGCCCAAAGGAAATC-3’ were synthesized and used in the qPCR reactions.

Statistical Analyses

Data are shown as the mean ± SD. Differences between groups were examined by 2-tailed Student’s *t* test or 2-way ANOVA for comparisons among multiple groups. For all analyses, $P < 0.05$ was considered statistically significant.

Supplementary Material

Refer to Web version on PubMed Central for supplementary material.

ACKNOWLEDGEMENTS

We are grateful for Drs. William Tu and Chunfang Zhu for their technical assistance. This work was supported by the NIH grants R01-CA070297, R01-CA151623, U01-CA166894, and R21-CA190021.

RERERENCES

1. Balk SP. Androgen receptor as a target in androgen-independent prostate cancer. Urology. 2002; 60:132–138. discussion 138–139. [PubMed: 12231070]
2. Gelmann EP. Molecular biology of the androgen receptor. J Clin Oncol. 2002; 20:3001–3015. [PubMed: 12089231]
3. Kyprianou N, Isaacs JT. Activation of programmed cell death in the rat ventral prostate after castration. Endocrinology. 1988; 122:552–562. [PubMed: 2828003]
4. Huggins C, Hodges CV. Studies on prostatic cancer: I. The effect of castration, of estrogen and of androgen injection on serum phosphatases in metastatic carcinoma of the prostate. 1941. J Urol. 2002; 168:9–12. [PubMed: 12050481]
5. Heinlein CA, Chang C. Androgen receptor in prostate cancer. Endocr Rev. 2004; 25:276–308. [PubMed: 15082523]
6. Koivisto P, Kononen J, Palmberg C, Tammela T, Hyytinen E, Isola J, et al. Androgen receptor gene amplification: a possible molecular mechanism for androgen deprivation therapy failure in prostate cancer. Cancer Res. 1997; 57:314–319. [PubMed: 9000575]

Author Manuscript Author Manuscript Author Manuscript Author Manuscript

7. Chen CD, Welsbie DS, Tran C, Baek SH, Chen R, Vessella R, et al. Molecular determinants of resistance to antiandrogen therapy. Nat Med. 2004; 10:33–39. [PubMed: 14702632]
8. Baca SC, Prandi D, Lawrence MS, Mosquera JM, Romanel A, Drier Y, et al. Punctuated evolution of prostate cancer genomes. Cell. 2013; 153:666–677. [PubMed: 23622249]
9. Verras M, Sun Z. Roles and regulation of Wnt signaling and beta-catenin in prostate cancer. Cancer Lett. 2006; 237:22–32. [PubMed: 16023783]
10. Sun Y, Campisi J, Higano C, Beer TM, Porter P, Coleman I, et al. Treatment-induced damage to the tumor microenvironment promotes prostate cancer therapy resistance through WNT16B. Nat Med. 2012; 18:1359–1368. [PubMed: 22863786]
11. Wissmann C, Wild PJ, Kaiser S, Roepcke S, Stoehr R, Woenckhaus M, et al. WIF1, a component of the Wnt pathway, is down-regulated in prostate, breast, lung, and bladder cancer. J Pathol. 2003; 201:204–212. [PubMed: 14517837]
12. Nusse R. Wnt signaling in disease and in development. Cell Res. 2005; 15:28–32. [PubMed: 15686623]
13. Amit S, Hatzubai A, Birman Y, Andersen JS, Ben-Shushan E, Mann M, et al. Axin-mediated CKI phosphorylation of beta-catenin at Ser 45: a molecular switch for the Wnt pathway. Genes Dev. 2002; 16:1066–1076. [PubMed: 12000790]
14. Hart MJ, de los Santos R, Albert IN, Rubinfeld B, Polakis P. Downregulation of beta-catenin by human Axin and its association with the APC tumor suppressor, beta-catenin and GSK3 beta. Curr Biol. 1998; 8:573–581. [PubMed: 9601641]
15. Latres E, Chiaur DS, Pagano M. The human F box protein beta-Trcp associates with the Cul1/Skp1 complex and regulates the stability of beta-catenin. Oncogene. 1999; 18:849–854. [PubMed: 10023660]
16. Aberle H, Bauer A, Stappert J, Kispert A, Kemler R. beta-catenin is a target for the ubiquitin-proteasome pathway. Embo J. 1997; 16:3797–3804. [PubMed: 9233789]
17. Chesire DR, Ewing CM, Gage WR, Isaacs WB. In vitro evidence for complex modes of nuclear beta-catenin signaling during prostate growth and tumorigenesis. Oncogene. 2002; 21:2679–2694. [PubMed: 11965541]
18. Gounari F, Signoretti S, Bronson R, Klein L, Sellers WR, Kum J, et al. Stabilization of beta-catenin induces lesions reminiscent of prostatic intraepithelial neoplasia, but terminal squamous transdifferentiation of other secretory epithelia. Oncogene. 2002; 21:4099–4107. [PubMed: 12037666]
19. Bierie B, Nozawa M, Renou JP, Shillingford JM, Morgan F, Oka T, et al. Activation of beta-catenin in prostate epithelium induces hyperplasias and squamous transdifferentiation. Oncogene. 2003; 22:3875–3887. [PubMed: 12813461]
20. Pearson HB, Phesse TJ, Clarke AR. K-ras and Wnt signaling synergize to accelerate prostate tumorigenesis in the mouse. Cancer Res. 2009; 69:94–101. [PubMed: 19117991]
21. Bruxvoort KJ, Charbonneau HM, Giambernardi TA, Goolsby JC, Qian CN, Zylstra CR, et al. Inactivation of Apc in the mouse prostate causes prostate carcinoma. Cancer Res. 2007; 67:2490–2496. [PubMed: 17363566]
22. Chesire DR, Ewing CM, Sauvageot J, Bova GS, Isaacs WB. Detection and analysis of beta-catenin mutations in prostate cancer. Prostate. 2000; 45:323–334. [PubMed: 11102958]
23. Gerstein AV, Almeida TA, Zhao G, Chess E, Shih Ie M, Buhler K, et al. APC/CTNNB1 (beta-catenin) pathway alterations in human prostate cancers. Genes Chromosomes Cancer. 2002; 34:9–16. [PubMed: 11921277]
24. Henrique R, Ribeiro FR, Fonseca D, Hoque MO, Carvalho AL, Costa VL, et al. High promoter methylation levels of APC predict poor prognosis in sextant biopsies from prostate cancer patients. Clin Cancer Res. 2007; 13:6122–6129. [PubMed: 17947477]
25. Chen Y, Li J, Yu X, Li S, Zhang X, Mo Z, et al. APC gene hypermethylation and prostate cancer: a systematic review and meta-analysis. Eur J Hum Genet. 2013; 21:929–935. [PubMed: 23299921]
26. Mulholland DJ, Cheng H, Reid K, Rennie PS, Nelson CC. The androgen receptor can promote beta-catenin nuclear translocation independently of adenomatous polyposis coli. J Biol Chem. 2002; 277:17933–17943. [PubMed: 11856748]

Author Manuscript Author Manuscript Author Manuscript Author Manuscript

27. Truica CI, Byers S, Gelmann EP. Beta-catenin affects androgen receptor transcriptional activity and ligand specificity. Cancer Res. 2000; 60:4709–4713. [PubMed: 10987273]
28. Yang F, Li X, Sharma M, Sasaki CY, Longo DL, Lim B, et al. Linking beta-catenin to androgen-signaling pathway. J Biol Chem. 2002; 277:11336–11344. [PubMed: 11792709]
29. Weischenfeldt J, Simon R, Feuerbach L, Schlangen K, Weichenhan D, Minner S, et al. Integrative genomic analyses reveal an androgen-driven somatic alteration landscape in early-onset prostate cancer. Cancer Cell. 2013; 23:159–170. [PubMed: 23410972]
30. Stanbrough M, Leav I, Kwan PW, Bubley GJ, Balk SP. Prostatic intraepithelial neoplasia in mice expressing an androgen receptor transgene in prostate epithelium. Proc Natl Acad Sci U S A. 2001; 98:10823–10828. [PubMed: 11535819]
31. Zhu C, Luong R, Zhuo M, Johnson DT, McKenney JK, Cunha GR, et al. Conditional expression of the androgen receptor induces oncogenic transformation of the mouse prostate. J Biol Chem. 2011; 286:33478–33488. [PubMed: 21795710]
32. Ittmann M, Huang J, Radaelli E, Martin P, Signoretti S, Sullivan R, et al. Animal models of human prostate cancer: the consensus report of the New York meeting of the Mouse Models of Human Cancers Consortium Prostate Pathology Committee. Cancer Res. 2013; 73:2718–2736. [PubMed: 23610450]
33. Muzumdar MD, Tasic B, Miyamichi K, Li L, Luo L. A global double-fluorescent Cre reporter mouse. Genesis. 2007; 45:593–605. [PubMed: 17868096]
34. Ding Z, Wu CJ, Chu GC, Xiao Y, Ho D, Zhang J, et al. SMAD4-dependent barrier constrains prostate cancer growth and metastatic progression. Nature. 2011; 470:269–273. [PubMed: 21289624]
35. Sauer L, Gitenay D, Vo C, Baron VT. Mutant p53 initiates a feedback loop that involves Egr-1/EGF receptor/ERK in prostate cancer cells. Oncogene. 2010; 29:2628–2637. [PubMed: 20190820]
36. Ellwood-Yen K, Graeber TG, Wongvipat J, Iruela-Arispe ML, Zhang J, Matusik R, et al. Myc-driven murine prostate cancer shares molecular features with human prostate tumors. Cancer Cell. 2003; 4:223–238. [PubMed: 14522256]
37. Mahmoudi T, Boj SF, Hatzis P, Li VS, Taouatas N, Vries RG, et al. The leukemia-associated Mllt10/Af10-Dot1l are Tcf4/beta-catenin coactivators essential for intestinal homeostasis. PLoS Biol. 2010; 8:e1000539. [PubMed: 21103407]
38. Chesire DR, Isaacs WB. Beta-catenin signaling in prostate cancer: an early perspective. Endocr Relat Cancer. 2003; 10:537–560. [PubMed: 14713266]
39. Heinlein CA, Chang C. Androgen receptor (AR) coregulators: an overview. Endocr Rev. 2002; 23:175–200. [PubMed: 11943742]
40. Wang Y, Revelo MP, Sudilovsky D, Cao M, Chen WG, Goetz L, et al. Development and characterization of efficient xenograft models for benign and malignant human prostate tissue. Prostate. 2005; 64:149–159. [PubMed: 15678503]
41. de Ronde JJ, Lips EH, Mulder L, Vincent AD, Wesseling J, Nieuwland M, et al. SERPINA6, BEX1, AGTR1, SLC26A3, and LAPTM4B are markers of resistance to neoadjuvant chemotherapy in HER2-negative breast cancer. Breast Cancer Res Treat. 2013; 137:213–223. [PubMed: 23203637]
42. Ibarretxe G, Aurrekoetxea M, Crende O, Badiola I, Jimenez-Rojo L, Nakamura T, et al. Epiprofin/Sp6 regulates Wnt-BMP signaling and the establishment of cellular junctions during the bell stage of tooth development. Cell Tissue Res. 2012; 350:95–107. [PubMed: 22868911]
43. Matusik RJ, Jin RJ, Sun Q, Wang Y, Yu X, Gupta A, et al. Prostate epithelial cell fate. Differentiation. 2008; 76:682–698. [PubMed: 18462434]
44. Wang X, Kruithof-de Julio M, Economides KD, Walker D, Yu H, Halili MV, et al. A luminal epithelial stem cell that is a cell of origin for prostate cancer. Nature. 2009; 461:495–500. [PubMed: 19741607]
45. Harada N, Tamai Y, Ishikawa T, Sauer B, Takaku K, Oshima M, et al. Intestinal polyposis in mice with a dominant stable mutation of the beta-catenin gene. Embo J. 1999; 18:5931–5942. [PubMed: 10545105]

Author Manuscript Author Manuscript Author Manuscript Author Manuscript

46. Wu X, Wu J, Huang J, Powell WC, Zhang J, Matusik RJ, et al. Generation of a prostate epithelial cell-specific Cre transgenic mouse model for tissue-specific gene ablation. Mech Dev. 2001; 101:61–69. [PubMed: 11231059]

47. Johnson DT, Luong R, Lee SH, Peng Y, Shaltouki A, Lee JT, et al. Deletion of leucine zipper tumor suppressor 2 (lzts2) increases susceptibility to tumor development. J Biol Chem. 2013; 288:3727–3738. [PubMed: 23275340]

48. Kwak MK, Johnson DT, Zhu C, Lee SH, Ye DW, Luong R, et al. Conditional deletion of the Pten gene in the mouse prostate induces prostatic intraepithelial neoplasms at early ages but a slow progression to prostate tumors. PLoS One. 2013; 8:e53476. [PubMed: 23308230]

49. Sugimura Y, Cunha GR, Donjacour AA. Morphological and histological study of castration-induced degeneration and androgen-induced regeneration in the mouse prostate. Biol Reprod. 1986; 34:973–983. [PubMed: 3730489]

50. Xin L, Ide H, Kim Y, Dubey P, Witte ON. In vivo regeneration of murine prostate from dissociated cell populations of postnatal epithelia and urogenital sinus mesenchyme. Proc Natl Acad Sci U S A. 2003; 100(Suppl 1):11896–11903. [PubMed: 12909713]

51. Hohaus S, Petrovick MS, Voso MT, Sun Z, Zhang DE, Tenen DG. PU.1 (Spi-1) and C/EBP alpha regulate expression of the granulocyte-macrophage colony-stimulating factor receptor alpha gene. Mol Cell Biol. 1995; 15:5830–5845. [PubMed: 7565736]

52. Livak KJ, Schmittgen TD. Analysis of relative gene expression data using real-time quantitative PCR and the 2(-Delta Delta C(T)) Method. Methods. 2001; 25:402–408. [PubMed: 11846609]

53. Lee J, Beliakoff J, Sun Z. The novel PIAS-like protein hZimp10 is a transcriptional co-activator of the p53 tumor suppressor. Nucleic Acids Res. 2007; 35:4523–4534. [PubMed: 17584785]

Author Manuscript Author Manuscript Author Manuscript Author Manuscript

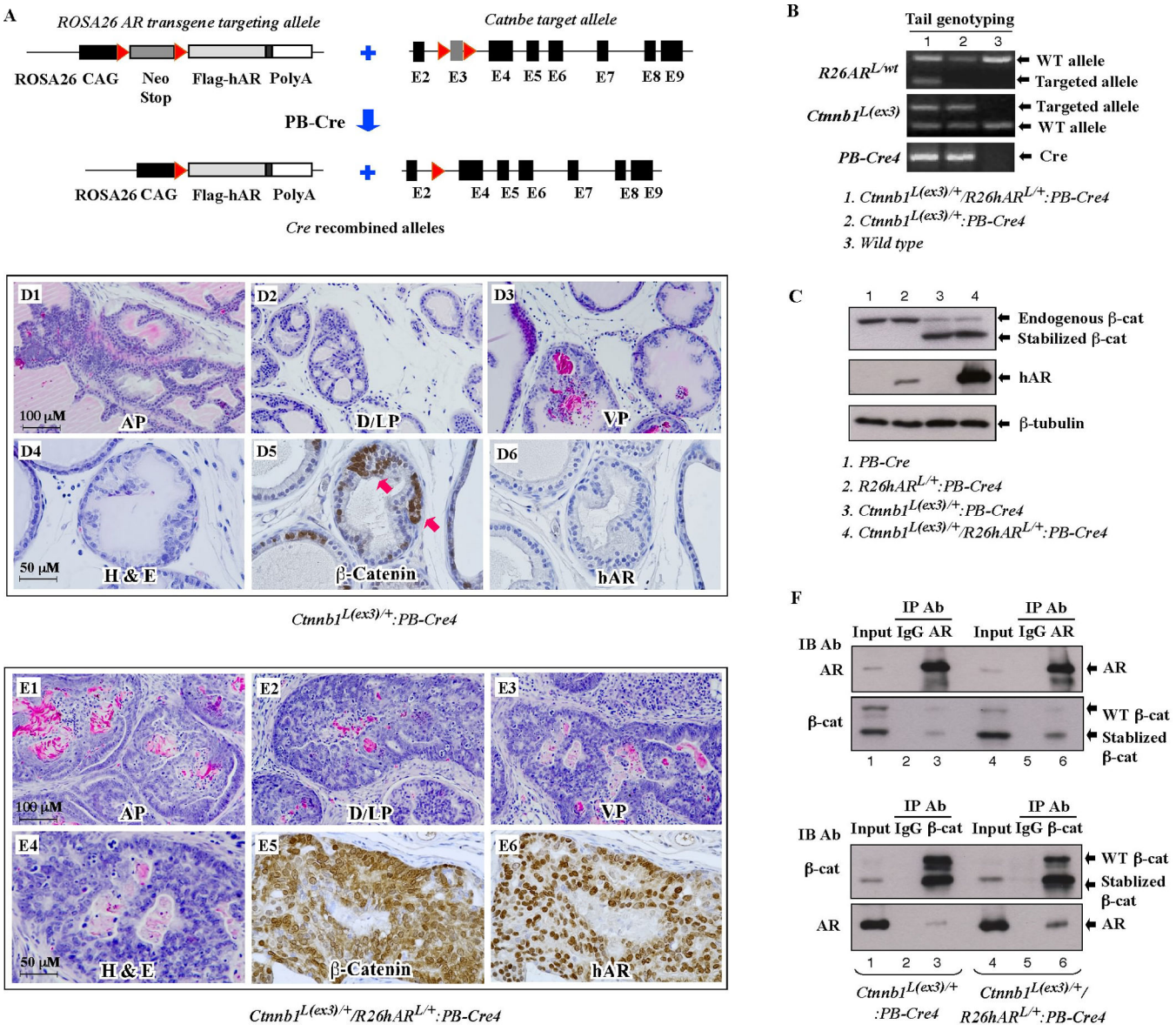

Figure 1. The conditional expression of human AR transgene and stabilized β-catenin allele in mouse prostate

A. A scheme of the conditional human AR transgene targeting construct is shown on a left figure. A PGK-neomycin cassette with flanked *loxP* sites (*LSL* cassettes) was inserted between the CAG promoter and a FLAG-tagged human AR coding sequence containing a nine-polyglutamine repeat tract. Red triangles sandwiching PGK-neomycin cassette (a dotted box) indicate *loxP* sequences. A targeting strategy for the exon 3 deletion of β-catenin gene is shown on a right figure. Exons are shown as filled boxes (E2–E9), whereas intronic sequences are shown as solid lines. Cre-recombined alleles for both constructs are shown below the targeting strategies. **B**. Genomic PCR was performed to confirm the targeting and *PB-Cre4* alleles using the tail tips of the mice. **C**. Western blotting was performed to confirm the protein expressions of stabilized β-catenin and transgenic human AR using prostate tissues isolated from the 8-week-old mice of the different genotypes. **D & E**. Low and high

Author Manuscript Author Manuscript Author Manuscript Author Manuscript

magnification photomicrographs of anterior prostate (AP), dorsal and lateral prostate (D/LP), and ventral prostate (VP) lobes from 5-weeks-old *Ctnnb1*$^{L(ex3)/+}$*:PB-Cre* and *Ctnnb1*$^{L(ex3)/+}$*/R26hAR*$^{L/+}$*:PB-Cre* mice stained with hematoxylin and eosin, or with the antibodies against β-catenin and human AR in which tissues were also counterstained with hematoxylin. Note the presence of low-grade mPIN lesions in the *Ctnnb1*$^{L(ex3)/+}$*:PB-Cre* mice (**D5** and **D6**) and high-grade mPIN lesions in *Ctnnb1*$^{L(ex3)/+}$*/R26hAR*$^{L/+}$*:PB-Cre* mice (**E5** and **E6**). **F**. Cell lysates from the prostate of 3-months-old *Ctnnb1*$^{L(ex3)/+}$*:PB-Cre* or *Ctnnb1*$^{L(ex3)/+}$*/R26hAR*$^{L/+}$*:PB-Cre* mice were immunoprecipitated with the AR (upper panel) or β-catenin antibody (lower panel), and analyzed by Western blotting (IB) with the indicated antibodies.

Author Manuscript Author Manuscript Author Manuscript Author Manuscript

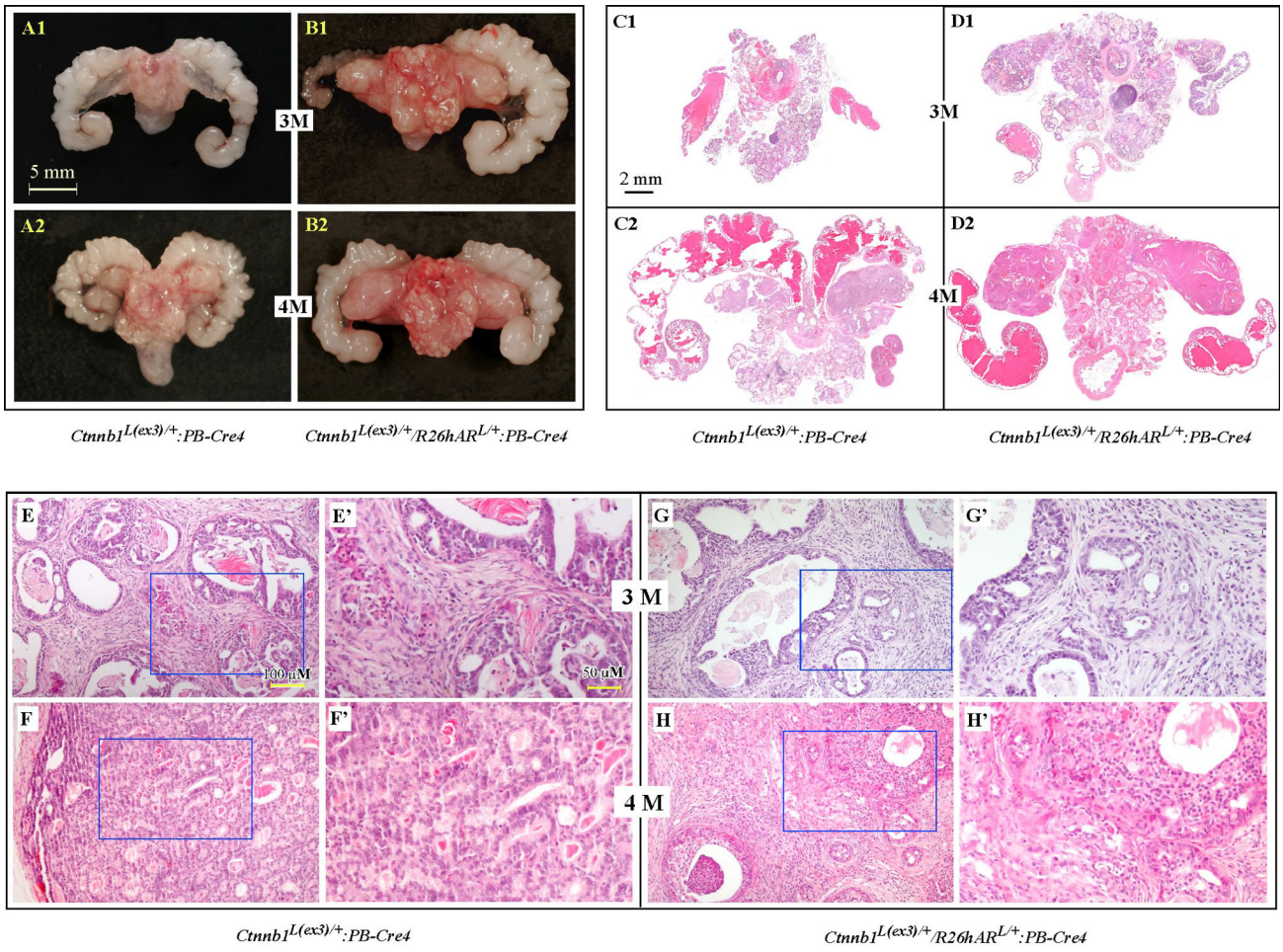

I. Pathological Abnormalities in the Prostates of β-catenin and AR Transgenic Mice

Genotypes	⩽ 1 month	> 1 month	> 2 months	> 4 months
Ctnnb1$^{L(ex3)/+}$/ *R26hAR*$^{L/+}$*:PB-Cre4*	4 of 4 LGPIN with scattered to multifocal HGPIN	4 of 4 multifocal intracystic adenocarcinoma with microinvasion	3 of 3 multifocal intracystic adenocarcinoma with extensive microinvasion plus early adenocarcinoma	4 of 4 massive intracystic adenocarcinoma with invasive adenocarcinoma
Ctnnb1$^{L(ex3)/+}$*:PB-Cre4*	3 of 3 scattered LGPIN	4 of 4 multifocal HGPIN	4 of 4 multifocal HGPIN with scattered intracystic adenocarcinoma	4 of 4 intracystic adenocarcinoma with no or rare invasion
R26hAR$^{L/+}$*:PB-Cre4*	4 of 4 normal	4 of 4 normal	5 of 5 normal	4 of 4 normal

Figure 2. The synergistic effect of AR and Wnt signaling in mouse prostate tumor progression

Corresponding gross photographs (**A1 to B2**), subgross photomicrographs (**C1 to D2**), and photomicrographs (**E to H**) of prostrate gland with seminal vesicles and urinary bladder from 3- to 4-month-old *Ctnnb1*$^{L(ex3)/+}$*:PB-Cre* and *Ctnnb1*$^{L(ex3)/+}$*/R26hAR*$^{L/+}$*:PB-Cre* mice. On the gross and subgross views, there is prostate adenocarcinoma development in both *Ctnnb1*$^{L(ex3)/+}$*:PB-Cre* and *Ctnnb1*$^{L(ex3)/+}$*/R26hAR*$^{L/+}$*:PB-Cre* mice, the tumors are larger in the *Ctnnb1*$^{L(ex3)/+}$*/R26hAR*$^{L/+}$*:PB-Cre* mice, based on volume and cross-sectional area). Microscopically, the tumors in both transgenic mice are represented by the development

Author Manuscript Author Manuscript Author Manuscript Author Manuscript

intracystic prostatic adenocarcinomas and high-grade mPIN lesions. In the *Ctnnb1*$^{L(ex3)/+}$*:PB-Cre* mice, there are few scattered intracystic prostatic adenocarcinomas with limited microinvasion into the surrounding stroma. In contrast, the larger tumors in the *Ctnnb1*$^{L(ex3)/+}$*/R26hAR*$^{L/+}$*:PB-Cre* mice correspond with the presence of larger numbers of intracystic prostatic adenocarcinomas with surrounding microstromal invasion. I. Pathological abnormalities in *R26hAR*$^{L/+}$*:PB-Cre*, *Ctnnb1*$^{L(ex3)/+}$*:PB-Cre*, and *Ctnnb1*$^{L(ex3)/+}$*/R26hAR*$^{L/+}$*:PB-Cre* mice.

Author Manuscript Author Manuscript Author Manuscript Author Manuscript

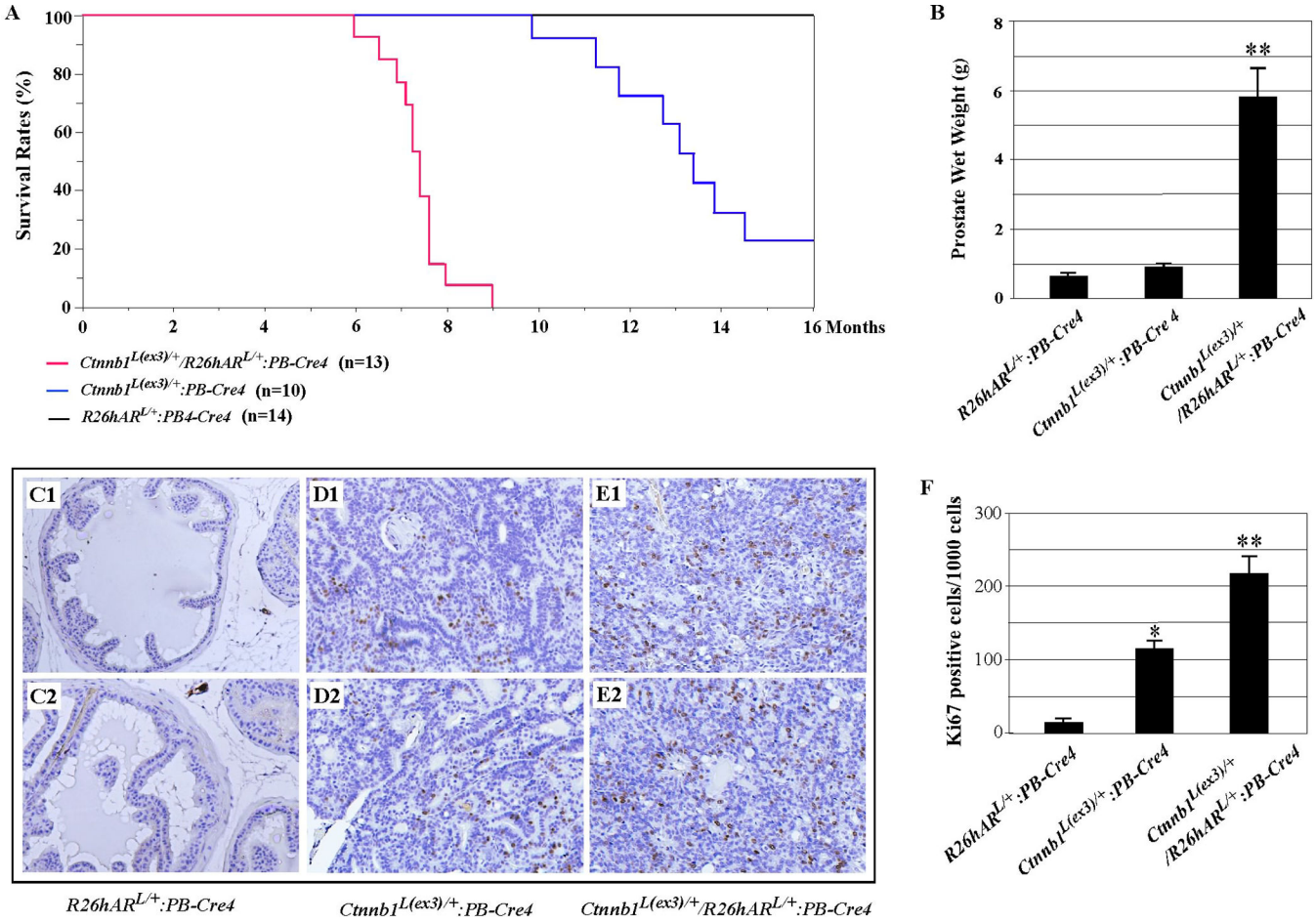

Figure 3. The mouse survival rate and prostatic cell proliferation

A. Kaplan–Meier survival curve of *Ctnnb1*$^{L(ex3)/+}$*/R26hAR*$^{L/+}$*:PB-Cre, Ctnnb1*$^{L(ex3)/+}$*:PB-Cre*, and *R26hAR*$^{L/+}$*:PB-Cre* mice. **B**. Wet weights of prostates of 7-month-old *R26hAR*$^{L/+}$*:PB-Cre, Ctnnb1*$^{L(ex3)/+}$*:PB-Cre*, and *Ctnnb1*$^{L(ex3)/+}$*/R26hAR*$^{L/+}$*:PB-Cre* mice. **, P <0.01. **C to E**. Prostate sections isolated from 3-month-old *R26hAR*$^{L/+}$*:PB-Cre, Ctnnb1*$^{L(ex3)/+}$*:PB-Cre*, and *Ctnnb1*$^{L(ex3)/+}$*/R26hAR*$^{L/+}$*:PB-Cre* mice were stained for Ki-67. **F**. A total of 1000 epithelial cells in each lesion from five different lesions from three mice of each genotype were evaluated for Ki-67 immunoreactivity. *, P <0.05, and **, P <0.01.

Author Manuscript Author Manuscript Author Manuscript Author Manuscript

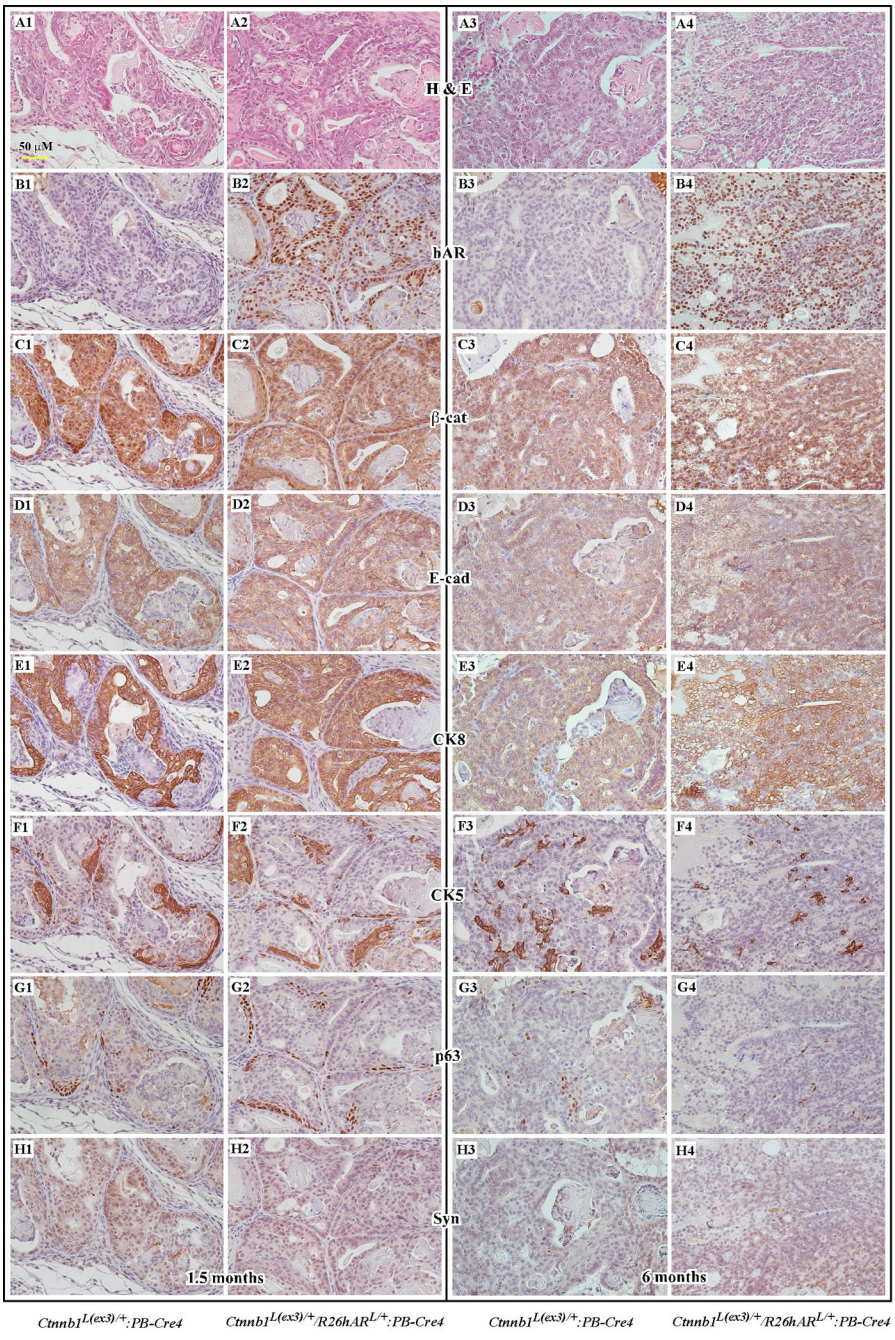

Figure 4. Immunohistochemistry analyses of the prostate tumors in *Ctnnb1$^{L(ex3)/+}$:PB-Cre* and *Ctnnb1$^{L(ex3)/+}$/R26hAR$^{L/+}$:PB-Cre* mice

Adjacent prostate tissue slides were prepared from prostatic tumor samples of 1.5- and 6-month-old *Ctnnb1$^{L(ex3)/+}$:PB-Cre* (**1** and **3**) and *Ctnnb1$^{L(ex3)/+}$/R26hAR$^{L/+}$:PB-Cre* mice (**2** and **4**). **A1–A4**, hematoxylin and eosin staining; **B1–H4**, immunohistochemistry with different antibodies as labeled in the figure.

Author Manuscript Author Manuscript Author Manuscript Author Manuscript

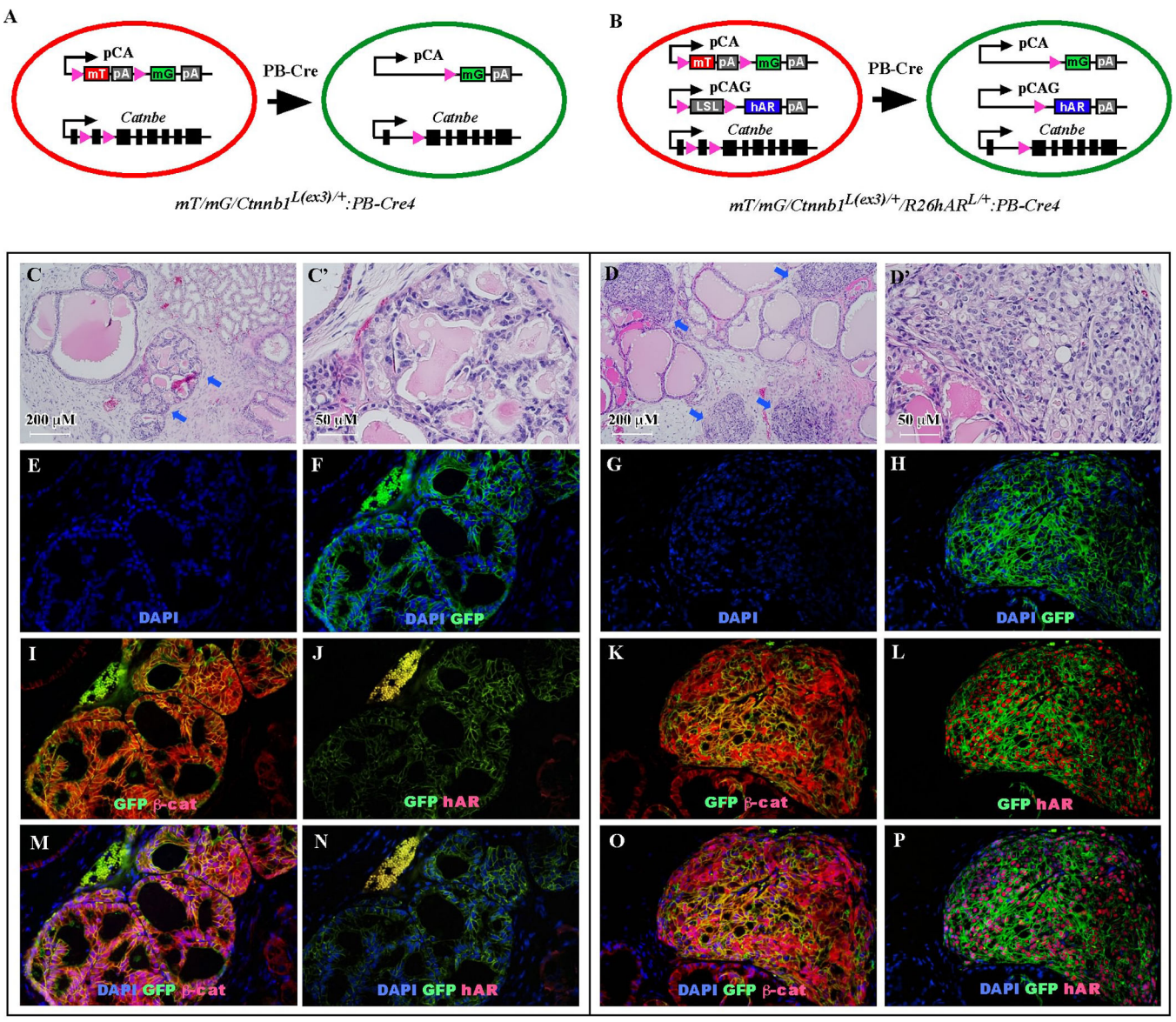

Figure 5. Regenerating activity of tumor cells from *mT/mG/Ctnnb1$^{L(ex3)/+}$:PB-Cre* and *mT/mG/Ctnnb1$^{L(ex3)/+}$/R26hAR$^{L/+}$:PB-Cre* prostates

A and B. Schematic illustration of labeling *PB-Cre* positive cells with the mT/mG reporter. **C–P**. Dissociated prostatic tumor cells from *mT/mG/Ctnnb1$^{L(ex3)/+}$/R26hAR$^{L/+}$:PB-Cre* and *mT/mG/Ctnnb1$^{L(ex3)/+}$:PB-Cre* mice were transplanted with urogenital sinus mesenchymal cells under the renal capsule in NOD/SCID mice. After 12 weeks, grafts were harvested and examined. **C to D**. H&E staining of the outgrown tissues. **E to P**. Immunofluorescent staining with different antibodies as labeled in the figure.

Author Manuscript Author Manuscript Author Manuscript Author Manuscript

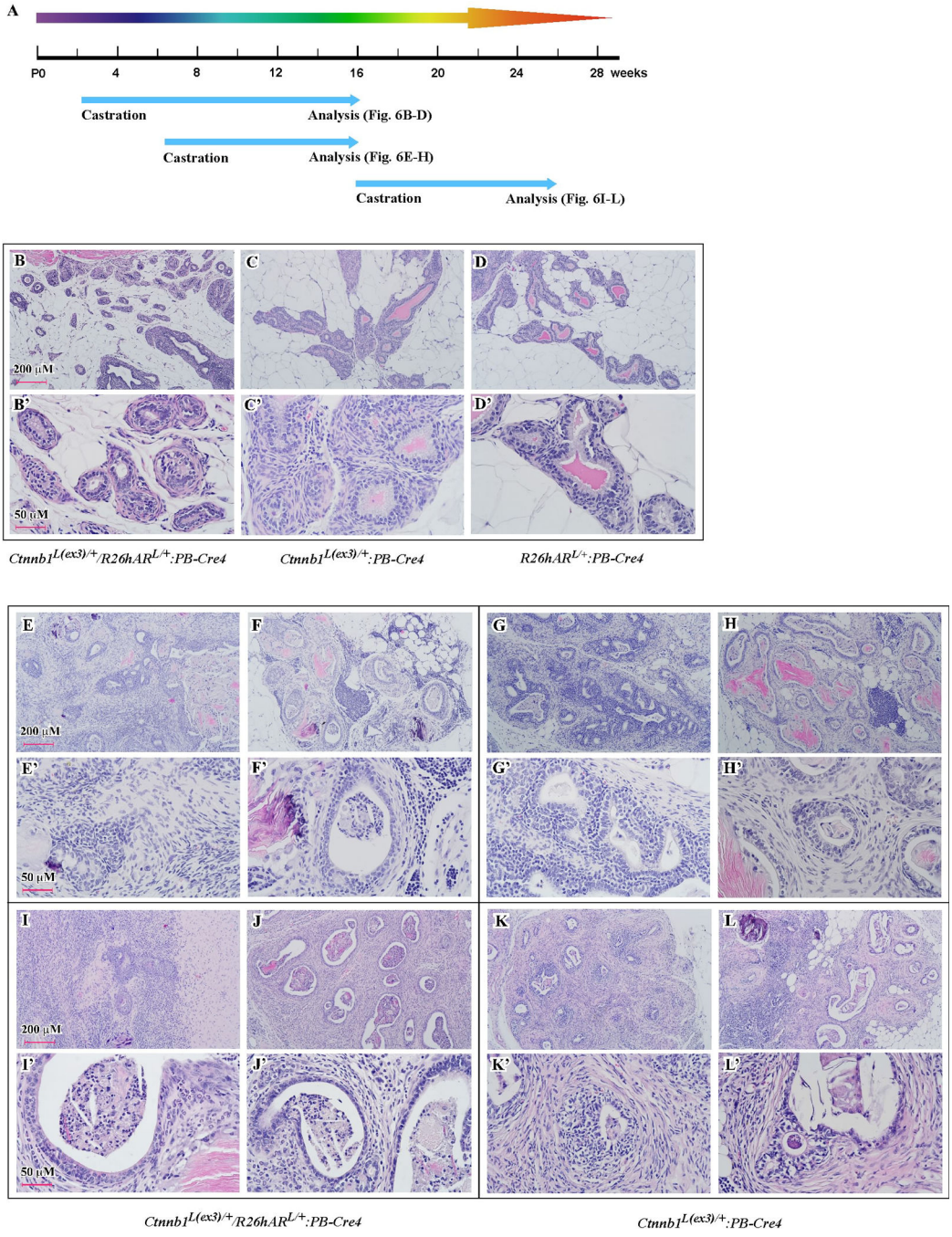

Figure 6. Androgen action is necessary for tumor formation and maintenance

A. Schematic illustration of castration. **B to D'**. Photomicrographs of prostate tissues from *Ctnnb1*$^{L(ex3)/+}$*/R26hAR*$^{L/+}$*:PB-Cre, Ctnnb1*$^{L(ex3)/+}$*:PB-Cre*, and *R26hAR*$^{L/+}$*:PB-Cre* mice castrated at 2 weeks and sacrificed at 16 wks, and stained with hematoxylin and eosin. Note the presence of only small numbers of prostate glandular profiles, which are widely scattered and of small diameter (interpreted as atrophy after hormone-withdrawal). **E to H'**. Photomicrographs of prostate tissues from *Ctnnb1*$^{L(ex3)/+}$*/R26hAR*$^{L/+}$*:PB-Cre* and *Ctnnb1*$^{L(ex3)/+}$*:PB-Cre* mice castrated at 6 wks and sacrificed at 16 wks, and stained with

Author Manuscript Author Manuscript Author Manuscript Author Manuscript

hematoxylin and eosin. The sections are highly cellular due mainly to the presence of abundant inflammation and fibroplasia, amongst which are small numbers of remnant prostate gland profiles. These glands are of small diameter and predominantly lined by a single or double layer of uniform, quiescent epithelial cells (interpreted as regression of mPIN lesions and/or prostatic adenocarcinoma lesions). Some remnant keratin and cellular/nuclear debris is present in the lumina of these glands. **I to L'**. Photomicrographs of prostate tissues from *Ctnnb1*$^{L(ex3)/+}$*/R26hAR*$^{L/+}$*:PB-Cre* and *Ctnnb1*$^{L(ex3)/+}$*:PB-Cre* mice castrated at 16 wks and sacrificed at 26 wks, and stained with hematoxylin and eosin. These sections appear similar to those noted in the *Ctnnb1*$^{L(ex3)/+}$*/R26hAR*$^{L/+}$*:PB-Cre* and *Ctnnb1*$^{L(ex3)/+}$*:PB-Cre* mice castrated at 6 wks, only differing by the additional presence of occasional prostatic glands that contain regressing mPIN lesions.

Author Manuscript Author Manuscript Author Manuscript Author Manuscript

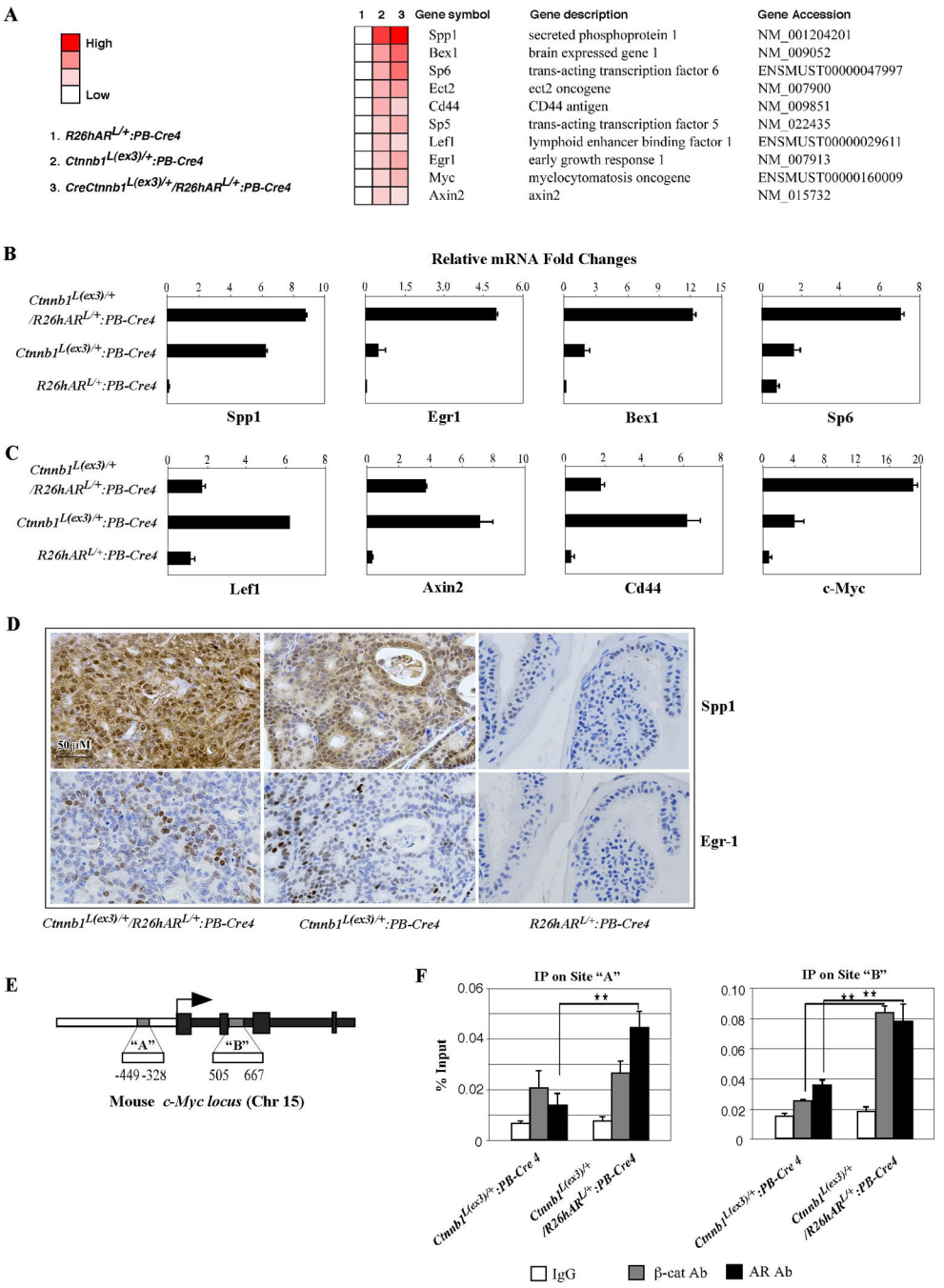

Figure 7. Co-expression of transgenic AR and stabilized β-catenin induces a subset of gene expression, which may contribute to prostate tumor initiation and progression

A. Gene microarray analysis showing the up-regulated genes in *Ctnnb1$^{L(ex3)/+}$:PB-Cre* and *Ctnnb1$^{L(ex3)/+}$/R26hAR$^{L/+}$:PB-Cre* prostates. RNAs extracted from 4-month-old *Ctnnb1$^{L(ex3)/+}$/R26hAR$^{L/+}$:PB-Cre, Ctnnb1$^{L(ex3)/+}$:PB-Cre*, and *R26hAR$^{L/+}$:PB-Cre* prostates were used for microarray analysis. **B to C**. qRT-PCR confirmation of the gene alterations in *Ctnnb1$^{L(ex3)/+}$:PB-Cre* and *Ctnnb1$^{L(ex3)/+}$/R26hAR$^{L/+}$:PB-Cre* prostates. **D**. Adjacent prostate tissue slides of 4-month-old *Ctnnb1$^{L(ex3)/+}$/R26hAR$^{L/+}$:PB-Cre,*

Author Manuscript Author Manuscript Author Manuscript Author Manuscript

Ctnnb1$^{L(ex3)/+}$*:PB-Cre*, and *R26hAR*$^{L/+}$*:PB-Cre* mice were stained with Spp1 and Egr-1 antibodies. **E**. Schematic representation of the mouse *c-Myc* locus containing two β-catenin/TCF4-binding regions. **F**. Cells isolated from prostate tissues of 3-month-old *Ctnnb1*$^{L(ex3)/+}$/*R26hAR*$^{L/+}$*:PB-Cre* and *Ctnnb1*$^{L(ex3)/+}$*:PB-Cre* mice were subjected to ChIP using β-catenin or AR antibodies, or normal IgG. Immunoprecipitated chromatin fragments were then analyzed by qPCR using specific primers for amplicon "A" (**7F**, left panel) and amplicon "B" (**7F**, right panel) spanning the mouse c-Myc locus as indicated in **E**. Results are presented as percentage immunoprecipitated over input. **, P <0.01